Anomalous phonon behavior in superconducting $CaKFe_4As_4$: An optical study

Run Yang,[1,2] Yaomin Dai,[2] Bing Xu,[3] Wei Zhang,[1] Ziyang Qiu,[1] Qiangtao Sui,[1] Christopher C. Homes,[2,*] and Xianggang Qiu[1,4,†]

[1]*Beijing National Laboratory for Condensed Matter Physics, Institute of Physics, Chinese Academy of Sciences, P.O. Box 603, Beijing 100190, China*

[2]*Condensed Matter Physics and Materials Science Division, Brookhaven National Laboratory, Upon, New York 11973, USA*

[3]*Center for High Pressure Science and Technology Advanced Research, Beijing 100094, China*

[4]*Collaborative Innovation Center of Quantum Matter, Beijing 100084, China*

(Received 14 October 2016; revised manuscript received 23 January 2017; published 8 February 2017)

The temperature dependence of *ab*-plane optical conductivity of $CaKFe_4As_4$ has been measured below and above its superconducting transition temperature $T_c \simeq 35.5$ K. In the normal state, analysis with the two-Drude model reveals a T-linear scattering rate for the coherent response, which suggests strong spin-fluctuation scattering. Below the superconducting transition, the optical conductivity below 120 cm^{-1} vanishes, indicating nodeless gap(s). The Mattis-Bardeen fitting in the superconducting state gives two gaps of $\Delta_1 \simeq 9$ meV and $\Delta_2 \simeq 14$ meV, in good agreement with recent angle-resolved photoemission spectroscopy (ARPES) results. In addition, around 255 cm^{-1}, we observe two different infrared-active Fe-As modes with obvious asymmetric lineshape, originating from strong coupling between lattice vibrations and spin or charge excitations. Considering a moderate Hund's rule coupling determined from spectral weight analysis, we propose that the strong fluctuations induced by the coupling between itinerant carriers and local moments may affect the phonon mode, and the electron-phonon coupling through the spin channel is likely to play an important role in the unconventional pairing in iron-based superconductors.

DOI: 10.1103/PhysRevB.95.064506

I. INTRODUCTION

The discrepancy between iron-based superconductors (FeSCs) and traditional BCS superconductors has prompted a great deal of effort to investigate their pairing mechanism [1–4]. Based on the strong magnetism in FeSCs [5], Mazin *et al.* proposed the $s_\pm$ pairing [6], which has a sign reversal in the gap function [7] and is mediated by spin fluctuations. In this scenario, the pairing state is fragile against nonmagnetic impurities. However, recent STM results on iron chalcogenides [8] are at odds with this scenario, supporting the sign-preserving pairing symmetry, i.e., s_{++} pairing, proposed by Kontani and Onari [9,10]. Electron-phonon coupling can induce strong orbital fluctuations, leading to an s_{++}-wave state with a high superconducting critical temperature (T_c) [11]. Although this scenario is consistent with several experimental results [8,12], it remains controversial. To provide new insights and construct a detailed model for the unconventional pairing in FeSCs, it is necessary to investigate materials with different crystal or electronic structures.

$CaKFe_4As_4$ is a member of the $AeAFe_4As_4$ (Ae stands for alkaline earth and A for alkali metal) family [13], which is a new system of FeSCs. Even though the chemical composition of $AeAFe_4As_4$ is the same as that of the heavily investigated $(Ae,A)Fe_2As_2$, the crystalline structure is rather different. In $(Ae,A)Fe_2As_2$, Ae^{2+} and A^+ randomly occupy crystallographically equivalent sites, while in $AeAFe_4As_4$, Ae^{2+} and A^+ stack alternatively across Fe_2As_2 layers, which not only increases the size of the unit cell but also changes the space group from $I4/mmm$ to $P4/mmm$. In addition, the lattice parameters of $AeAFe_4As_4$ lie between those of $AeFe_2As_2$ and AFe_2As_2. Therefore, $AeAFe_4As_4$ could be regarded as the hybrid phase of $AeFe_2As_2$ and AFe_2As_2. In the $AeAFe_4As_4$ family, most compounds have a T_c between 31–36 K. Most recently, similar materials $RbGd_2Fe_4As_4O$ and $KCa_2Fe_4As_4F_2$ have been synthesized with superconductivity at $T_c = 33$ K [14,15]. These two compounds, together with the $AeAFe_4As_4$ family, are regarded as the hybrid phase between the iron-based parent compounds and AFe_2As_2. An open question is: What is the possible driving mechanism for high-T_c superconductivity in these materials? Investigating this can help us to understand the possible unconventional pairing in the FeSCs.

In this work, we have synthesized high-quality single crystals of $CaKFe_4As_4$ with T_c of 35.5 K. The detailed temperature dependence of the complex optical properties in the *ab* plane, above and below T_c, has been obtained from reflectivity measurements. In the normal state, like most iron pnictides, the real part of the optical conductivity can be described quite well by the two-Drude model, while in the superconducting (SC) state, a clear signature of nodeless SC gaps are observed. The onset of the absorption occurs around 120 cm^{-1} in the optical conductivity. Fitting the optical conductivity with Marttis-Bardeen formalism yields two SC gaps, $\Delta_1 \simeq 9$ meV and $\Delta_2 \simeq 14$ meV, which agree well with recent ARPES studies [16]. The optical properties are very similar to those of $Ba_{0.6}K_{0.4}Fe_2As_2$ [17,18]. However, in $CaKFe_4As_4$, two in-plane infrared-active modes are observed, which are associated with two different Fe-As bonds, in contrast to only one Fe-As mode in other iron pnictides [19,20]. Comparing with $CaFe_2As_2$ and KFe_2As_2, we find signatures of enhanced electron-phonon coupling in $CaKFe_4As_4$. Moreover, the spectral-weight analysis points to a moderate Hund's rule coupling in $CaKFe_4As_4$. We propose that in $CaKFe_4As_4$,

*homes@bnl.gov
†xgqiu@iphy.ac.cn

electrons may couple to the phonons through the spin channel [21], which is likely to play an important role in unconventional pairing in $CaKFe_4As_4$.

II. EXPERIMENT

High-quality single crystals of $CaKFe_4As_4$ with good cleavage planes (001) were synthesized using the self-flux method [14]. Resistivity measurement was carried out on a Quantum Design physical property measurement system (PPMS). The dc magnetic susceptibility was measured using a Quantum Design superconducting quantum interference device (SQUID). The reflectivity from the cleaved surface has been measured at a near-normal angle of incidence on Fourier transform infrared spectrometers (Bruker 80v and IFS 113v) for light polarized in the *ab* plane using an *in situ* evaporation technique [22]. Data from 30 to 15 000 cm^{-1} were collected at different temperatures from 5 to 295 K with the sample mounted on an ARS Helitran cryostat. The reflectivity in the visible and UV range (10 000–40 000 cm^{-1}) at room temperature was taken with an Avaspec 2048 × 14 optical fiber spectrometer. The optical conductivity has been determined from a Kramers-Kronig analysis of the reflectivity $R(\omega)$ over the entire frequency range. Since the measurement is taken in a limited energy range, a Hagen-Rubens relation ($R = 1 - A\sqrt{\omega}$) is used for the low-frequency ($\lesssim 30$ cm^{-1}) extrapolation, while in the SC state the relation ($R = 1 - A\omega^4$) is used to extrapolate the low frequency data [17]. Above the highest-measured frequency (40 000 cm^{-1}), $R(\omega)$ is assumed to be constant up to 40 eV, above which a free-electron response (ω^{-4}) is used.

III. RESULTS AND DISCUSSION

A. Normal and superconducting state

Figure 1 (main panel) shows the temperature dependence of the resistivity and magnetic susceptibility, from which

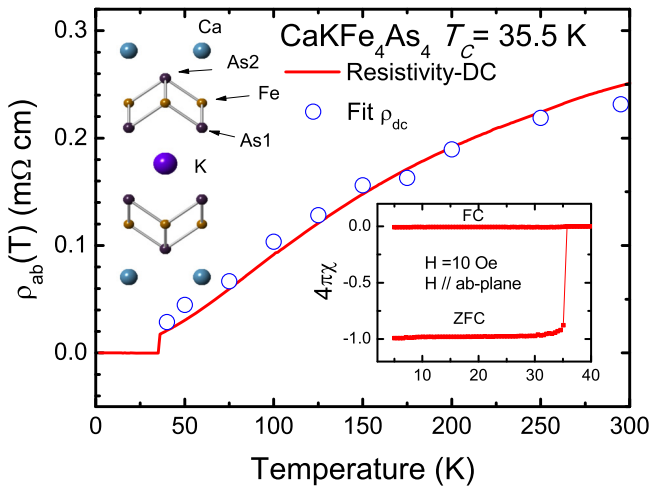

FIG. 1. Temperature dependence of resistivity of $CaKFe_4As_4$, the blue circles denote the zero-frequency extrapolation of its optical conductivity. The lower inset shows the magnetic susceptibility of the sample (χ represents the magnetic susceptibility per unit volume). Both of them show a sharp superconducting transition at $T_c = 35.5$ K. The upper inset shows the lattice structure of $CaKFe_4As_4$; there are two different Fe-As bonds in one FeAs layer.

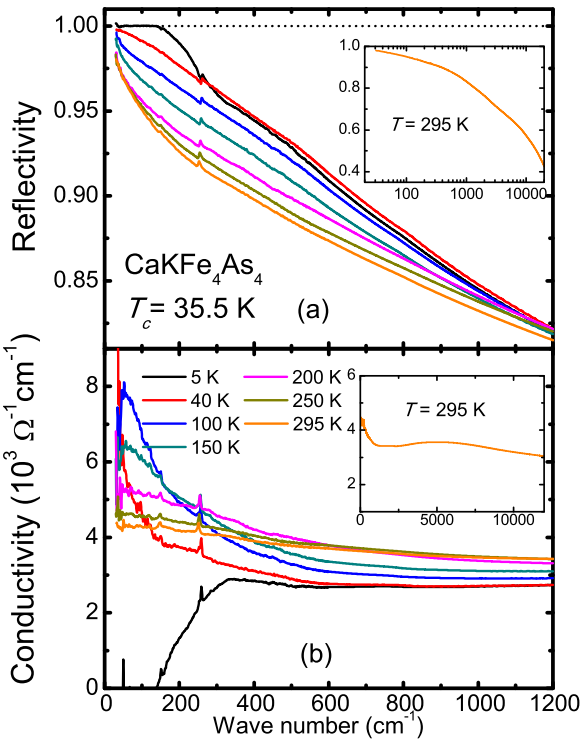

FIG. 2. (a) Reflectivity (b) and optical conductivity of $CaKFe_4As_4$ at various temperatures above and below the superconducting transition. The insets are the data in a larger energy area.

we observe a sharp SC transition at 35.5 K. The value of $4\pi\chi = -1$ at $T \ll T_c$ indicates the bulk superconductivity. The measured *ab*-plane reflectivity $R(\omega, T)$ and the real part of the optical conductivity $\sigma_1(\omega, T)$ for selected temperatures below and above the SC transition are summarized in Fig. 2. In the normal state, the high reflectivity at low frequency (<1000 cm^{-1}) which increases upon cooling reflects the metallic nature of the materials [23]. Below T_c, the reflectivity shows a sudden up-turn and reaches unity with a flat response below 120 cm^{-1}. Similar behavior has also been observed in $Ba_{0.6}K_{0.4}Fe_2As_2$ which is attributed to the formation of a superconducting energy gap or gaps [17,18]. Correspondingly, in the optical conductivity at low temperature (5 K), the optical absorption vanishes below 120 cm^{-1}, indicating the opening of nodeless SC gaps.

To quantitatively analyze the optical properties of $CaKFe_4As_4$, we fit the $\sigma_1(\omega, T)$ with a simple Drude-Lorentz model for the dielectric function [23,24],

$$\epsilon(\omega) = \epsilon_\infty - \sum_j \frac{\Omega_{p,j}^2}{\omega^2 + i\omega/\tau_j} + \sum_k \frac{\Omega_k^2}{\omega_k^2 - \omega^2 - i\omega/\tau_k}, \quad (1)$$

where ϵ_∞ is the real part of the dielectric function at high frequency; the second term describes a sum of free-carrier Drude responses characterized by a plasma frequency $\Omega_{p,j}^2 = 4\pi n_j e^2/m_j^*$, with n_j the carrier concentration, m_j^* the effective mass, and $1/\tau_j$ the scattering rate. The third term is a sum of Lorentz oscillators characterized by a resonance frequency ω_k, a linewidth γ_k, and an oscillator strength Ω_k. The fitting

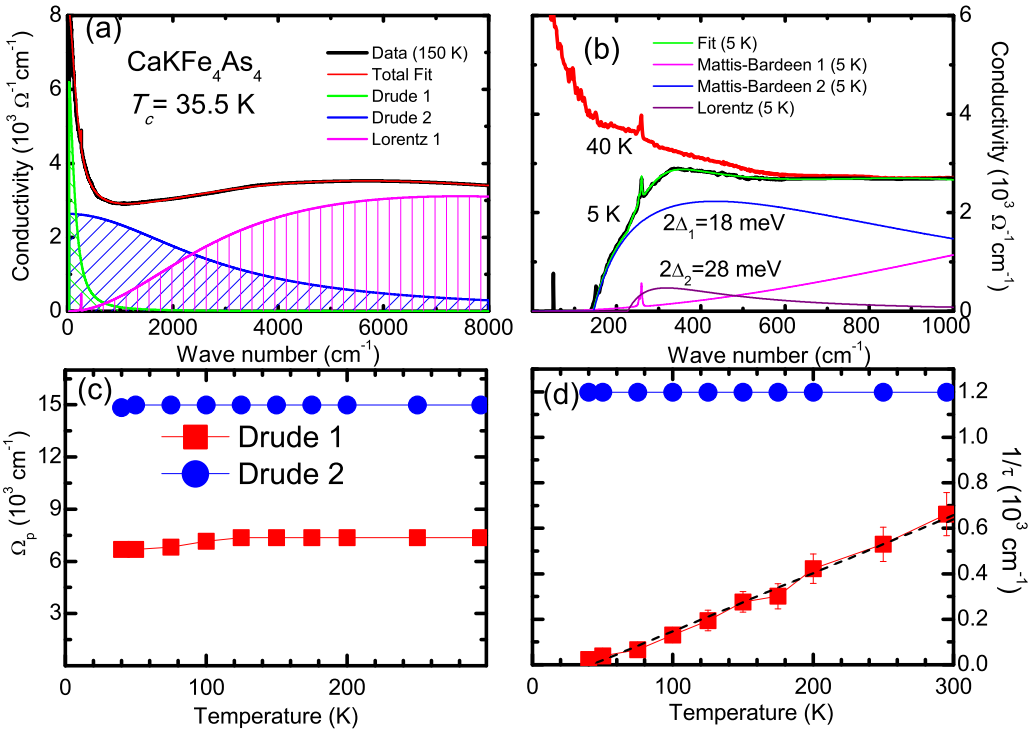

FIG. 3. (a) Optical conductivity of $CaKFe_4As_4$ at 150 K (thick black lines), fitted with the Drude-Lorentz model (thin red lines) and its decomposition into individual Drude and Lorentz terms. (b) The optical conductivity of $CaKFe_4As_4$ in the SC state is fit using the Mattis-Bardeen formalism, which results in two SC gaps with the size of $\Delta_1 \simeq 9 \pm 0.2$ meV and $\Delta_2 \simeq 14 \pm 0.5$ meV. (c) The plasma frequency Ω_p and (d) scattering rate $1/\tau$ for the narrow Drude (red); broad Drude (blue) components are extracted by fitting the data at various temperatures in the normal state.

of the normal state at 150 K is shown in Fig. 3(a). As in most iron pnictides, the optical response of $CaKFe_4As_4$ below 8000 cm^{-1} can be described by a narrow Drude (a coherent response), a broad Drude (an incoherent response), and a Lorentz term (interband transition) [25,26], reflecting the multiband nature of FeSCs. With this fitting, we extrapolate the optical conductivity to the zero frequency and find that the extrapolation agree well with the resistivity (Fig. 1), indicating that the two-Drude mode can well describe the nature of $CaKFe_4As_4$. From the fitting results [Figs. 1(c) and 1(d)], we notice that the scattering rate and plasma frequency of the broad Drude term are almost temperature independent, while the scattering rate of the narrow Drude component shows an obvious T-linear behavior, indicating strong spin-fluctuation scattering [23,27].

In the SC state, since the optical conductivity in the low-frequency range (<500 cm^{-1}) is significantly suppressed due to the opening of the SC gaps, the Mattis-Bardeen formalism has been used to describe the optical response. As shown in Fig. 3(b), two SC gaps and a Lorentz component reproduce the experimental data quite well. These two gaps are determined to be $\Delta_1 \simeq 9 \pm 0.2$ meV and $\Delta_2 \simeq 14 \pm 0.5$ meV, in good agreement with those obtained by ARPES measurements [16]. The strong reduction of the conductivity at low frequency for $T \ll T_c$ suggests the absence of nodes. Our optical results provide estimates of the gap amplitudes but cannot give direct evidence to distinguish between s± and extend s-wave pairing.

In the superconducting state, a large fraction of the itinerant carriers have condensed into the superfluid. To estimate the superfluid density, we have used the Ferrell-Glover-Tinkham (FGT) sum rule to calculate the missing area between the conductivity at $T \simeq T_c$ and $T \ll T_c$ [17],

$$\omega_{ps}^2 = 8 \int_{0^+}^{\omega_c} [\sigma_1(\omega, T \simeq T_c) - \sigma_1(\omega, T \ll T_c)] d\omega, \qquad (2)$$

where $\omega_{ps} = \sqrt{4\pi n_s e^2/m^*}$ is the superconducting plasma frequency, n_s represents the superfluid density, and $\omega_c = 600$ cm^{-1} is a cutoff frequency at which the optical conductivity shows no difference between 40 and 5 K data. The calculation yields the superconducting plasma frequency $\omega_{ps} \simeq 8065 \pm 200$ cm^{-1} and the corresponding penetration depth $\lambda = 1/2\pi\omega_{ps} \approx 2\,000$ Å.

B. Phonon anomalies

Two sharp peaks representing the symmetry allowed ab-plane infrared-active E_u modes are observed around 255 cm^{-1} [Fig. 4(a)]. Similar features are also found around the same energy area in other iron pnictides [20]. However, there are two modes in $CaKFe_4As_4$, in contrast to the only one mode in other related pnictides. Since this mode is assigned to the in-plane displacement of the Fe and As atoms [23], taking the lattice structure of $CaKFe_4As_4$ into consideration, we infer that these two modes originate from Fe-As bonds with different bond lengths. The mode at lower frequency (phonon A) corresponds to the longer Fe-As(1) bond (see the upper inset of Fig. 1) with a length of 2.395 Å, while the other mode (phonon B)

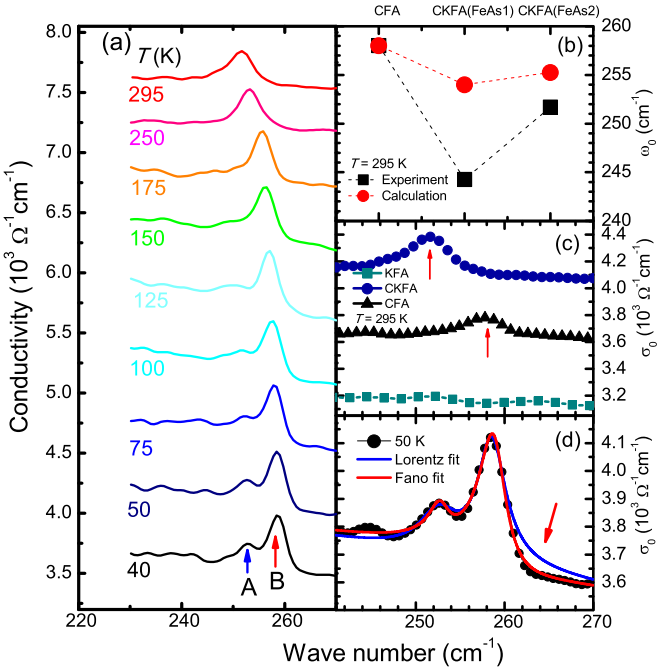

FIG. 4. (a) The real part of the optical conductivity of $CaKFe_4As_4$ above and below $T_c \simeq 35.5$ K in the region of the infrared-active mode around 255 cm^{-1}, from which we observe two different phonon modes. (b) The black squares denote the resonance frequency ω_0 of the Fe-As mode at 295 K for $CaFe_2As_2$ and $CaKFe_4As_4$; the red circles denote the calculated frequency based on the Fe-As bond length. (c) The phonon modes in $CaKFe_4As_4$ (CKFA), $CaFe_2As_2$ (CFA), and KFe_2As_2 (KFA) at 295 K, from which we observe the softening and enhancement of the phonon in $CaKFe_4As_4$. (d) The fitting to the phonon modes in $CaKFe_4As_4$ at 50 K with a Fano and a Lorentz model, from which we observe a discrepancy for the Lorentz fit (indicated by the arrow), while the Fano model gives a better result.

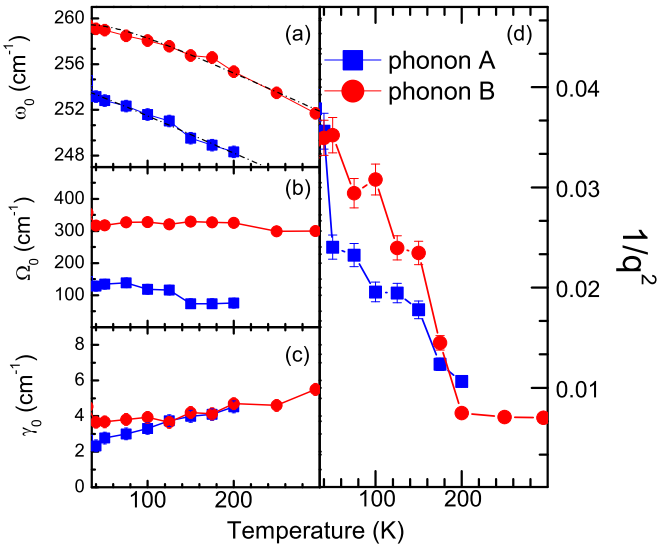

FIG. 5. The temperature dependence of the (a) infrared-active mode compared with the anharmonic decay model (dashed dotted line), (b) oscillator strength, (c) asymmetry parameter, and (d) linewidth.

corresponds to the Fe-As(2) bond with a shorter bond length of 2.387 Å [13].

Considering the fact that $CaKFe_4As_4$ can be regarded as the hybrid phase of $CaFe_2As_2$ and KFe_2As_2, as shown in Fig. 4(c), we compare the phonon modes of these three materials. We find that in KFe_2As_2 the phonon is indiscernible; it may be due to its heavy hole concentration or the extremely high density of states near the Fermi level [28]. Compared with $CaFe_2As_2$, both of these two phonon modes in $CaKFe_4As_4$ shift to lower frequencies (softening) [29]. This may originate from the elongated FeAs bonds. With a simple formula $\omega_0/\omega_0' = (l'/l)^{3/2}$ (ω_0 represents the resonance frequency; l is the bond length) [30], we can estimate the frequency shifts of the phonon modes in $CaKFe_4As_4$ with respect to that in $CaFe_2As_2$ due to the elongated Fe-As bond length [results are shown in Fig. 4(b)]. We find that the experimental data is much smaller than the calculated ones. This fact suggests that the elongation of the FeAs bonds alone cannot account for the softening of the phonon in $CaKFe_4As_4$.

In some other materials, such as $Sr_{1-x}Ba_xCu_2(BO_3)_2$ [31,32] and gate-tuned bilayer graphene [33], phonon softening has also been observed and attributed to spin-phonon and electron-phonon coupling, respectively. Moreover, in iron-based superconductors, spin- or electron-phonon coupling have been predicted by theoretical calculations [21] and later observed in experimental researches in some other pnictides [20,34]. Therefore, the spin- or electron-phonon coupling may be responsible for the extra phonon softening in $CaKFe_4As_4$.

To test this prediction, we investigate the lineshape of the phonons, since the coupling of the lattice to either the spin or electron background may give rise to an asymmetric lineshape [34,35]. If there is no coupling, the phonon mode shows a symmetric lineshape, which can be fitted with a Lorentz oscillator. In Fig. 4(d), we find that the Lorentz fitting for the phonon modes is poor. In order to improve the fitting, we employ the Fano line shape [34,35],

$$\sigma_1(\omega) = \frac{2\pi}{Z_0}\frac{\Omega^2}{\gamma}\frac{q^2 + \frac{4q(\omega-\omega_0)}{\gamma} - 1}{q^2\left(1 + \frac{4(\omega-\omega_0)^2}{\gamma}\right)}, \quad (3)$$

where ω_0, γ, and Ω represent the resonance frequency, linewidth, and strength of the phonon, and Z_0 is the vacuum impedance,which equals to 377 Ω. The asymmetry of the lineshape is described by $1/q^2$. As $1/q^2$ increases, the lineshape becomes increasingly asymmetric, indicating an enhanced coupling. As $1/q^2 \to 0$, a symmetric Lorentzian lineshape is recovered.

The temperature dependence of these two phonons has been analyzed using two asymmetric Fano modes with a Drude-Lorentz background. The results are summarized in Fig. 5. We note that upon cooling, the frequency of these two modes, as shown in Fig. 5(a), shifts to a higher frequency (hardens), a tendency that can be described by the anharmonic decay model [36]. The strength of these two modes [Fig. 5(b)] both increase with decreasing temperature, while the linewidths [Fig. 5(d)] decrease monotonically with temperature. The asymmetry parameter $1/q^2$ [Fig. 5(c)] is very small (<0.01) at room temperature, but largely enhanced at low temperatures, indicating increasing spin- or electron-phonon coupling [20,34]. Furthermore, while the behavior of these two modes

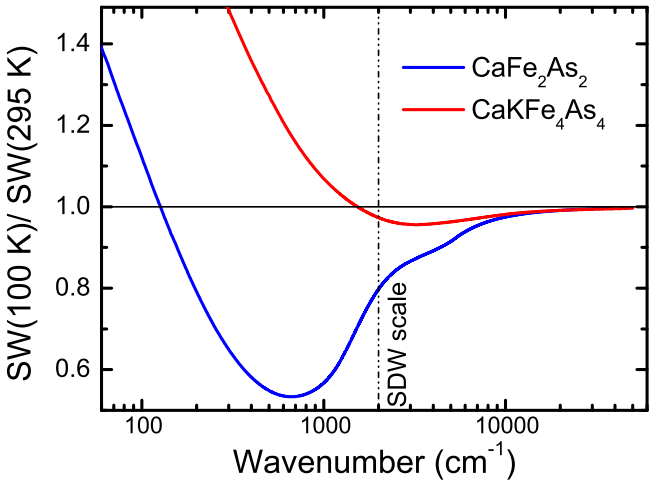

FIG. 6. Ratio of the integrated spectral weight SW(100 K)/SW(295 K), where SW $= \int_0^{\omega_c} \sigma_1(\omega) d\omega$, as a function of the cutoff frequency ω_c, in $CaFe_2As_2$ and $CaKFe_4As_4$.

is similar, they are in different amplitudes. The phonon mode corresponding to the Fe-As(2) bond (phonon B) is stronger than the one that corresponds to the Fe-As(1) bond (phonon A), indicating stronger coupling to the shorter Fe-As bond.

C. Spectral weight analysis

We have also carried out the spectral weight analysis in $CaFe_2As_2$ and $CaKFe_4As_4$. In Fig. 6, the low-temperature spectral weight of these two materials has been normalized to the integrated spectral weight at room temperature. We observe that in both materials, at low temperatures, the spectral weight at low frequency ($\lesssim$1000 cm^{-1}) is suppressed and gradually recovers at roughly 12 000 cm^{-1}; such behavior is widely ascribed to the Hund's rule coupling effect [37], by which the itinerant carriers are localized and polarized by the local moment. Nevertheless, compared with $CaFe_2As_2$, the spectral weight transfer is weaker in $CaKFe_4As_4$, and in KFe_2As_2 the spectral weight transfer tends to vanish [37]. As Wang *et al.* [37] pointed out, with increasing K doping, the pnictogen height relative to the Fe layer (h_{As}) increases. As a result, the Hund's rule coupling is enhanced [38,39], so that most of the itinerant carriers are localized at high temperature and the spectral weight transfer could not be seen from room temperature down to 5 K. Since the pnictogen height of $CaKFe_4As_4$ (1.41 Å) is between that of $CaFe_2As_2$ (1.37 Å) and KFe_2As_2 (1.42 Å), we infer that the Hund's coupling effect in $CaKFe_4As_4$ also lies between that of $CaFe_2As_2$ and KFe_2As_2.

Very recently, Tam *et al.* [40] pointed out that with Hund's rule coupling, the itinerant carriers with a well-nested Fermi surface can couple with the local moment and induce large spatial and temporal quantum fluctuations. In $CaFe_2As_2$, owing to the lower pnictogen height, Hund's coupling is relatively weak. On the contrary, in KFe_2As_2, although the Hund's coupling is strong, the heavy concentration of holes eliminates the nesting of the Fermi surface [41]. In $CaKFe_4As_4$, the hybridization between $CaFe_2As_2$ and KFe_2As_2 will dilute the hole concentration in KFe_2As_2, leading to a well-nested Fermi surface [27,40], and a higher pnictogen height results in a stronger Hund's rule coupling than $CaFe_2As_2$. These two factors give rise to strong quantum fluctuations, resulting in the T-linear scattering rate of the coherent response [42], which has been regarded as an important ingredient for unconventional pairing. Since the itinerant carriers deliver the superexchange interaction through Fe-As bond, and the phonon mode modifies the electron hopping [43], we suggest that the fluctuations of the local moment may also somehow influence the phonon mode, resulting in an enhanced electron-phonon coupling. Moreover, since the charge transfer prefers the shorter Fe-As bond, the corresponding phonon may exhibit stronger coupling. This could explain the different behaviors of these two phonon modes in $CaKFe_4As_4$.

IV. SUMMARY

In summary, the detailed optical properties of $CaKFe_4As_4$ have been determined above and below $T_c \approx 35.5$ K. In the superconducting state two gaps of 9 and 14 meV have been determined, which suggests an s-wave pairing symmetry. Additionally, we have identified two infrared-active Fe-As phonons around 255 cm^{-1}. In comparison with $CaFe_2As_2$ and KFe_2As_2, we find clear signatures of spin- or electron-phonon coupling in these two modes. We propose that in $CaKFe_4As_4$, the strong quantum fluctuations induced by the itinerant carriers with a well-nested Fermi surface through the Hund's rule coupling may affect the vibration of the Fe-As bond through spin-lattice coupling. Considering the large isotope effect in $SmFeAsO_{1-x}F_x$ and $Ba_{1-x}K_xFe_2As_2$ [44], we suggest that even though the magnetism plays an important role, the electron-phonon coupling should also be considered in the investigation of the superconductivity of iron-based superconductors.

ACKNOWLEDGMENTS

We thank Congcong Le, Xianxin Wu, Huiqian Luo, Guodong Liu, Bohong Li, Fei Cheng, and Kashif Nadeem for useful discussions. Work at Chinese Academy of Science was supported by NSFC (Projects No. 11374345 and No. 91421304) and MOST (Projects No. 2015CB921303 and No. 2015CB921102). Work at Brookhaven National Laboratory was supported by the Office of Science, U.S. Department of Energy under Contract No. DE-SC0012704.

[1] D. Christianson, E. Goremychkin, R. Osborn, S. Rosenkranz, M. D. Lumsden, C. D. Malliakas, I. S. Todorov, H. Claus, D. Y. Chung, M. G. Kanatzidis, R. I. Bewley, and T. Guidi, Unconventional superconductivity in $Ba_{0.6}K_{0.4}Fe_2As_2$ from inelastic neutron scattering, Nature (London) **456**, 930 (2008).

[2] Clarina de la Cruz, Q. Huang, J. W. Lynn, J. Li, W. Ratcliff II, J. L. Zarestky, H. A. Mook, G. F. Chen, J. L. Luo, N. L. Wang, and P. Dai, Magnetic order close to superconductivity in the iron-based layered $LaO_{1-x}F_xFeAs$ systems, Nature (London) **453**, 899 (2008).

[3] H. Takahashi, K. Igawa, K. Arii, Y. Kamihara, M. Hirano, and H. Hosono, Superconductivity at 43 K in an iron-based layered compound $LaO_{1-x}F_xFeAs$, Nature (London) **453**, 376 (2008).

[4] X. Chen, P. Dai, D. Feng, T. Xiang, and F.-C. Zhang, Iron-based high transition temperature superconductors, Nat. Sci. Rev. **1**, 371 (2014).

[5] M. D. Johannes and I. I. Mazin, Microscopic origin of magnetism and magnetic interactions in ferropnictides, Phys. Rev. B **79**, 220510 (2009).

[6] I. I. Mazin, D. J. Singh, M. D. Johannes, and M. H. Du, Unconventional Superconductivity with a Sign Reversal in the Order Parameter of $LaFeAsO_{1-x}F_x$, Phys. Rev. Lett. **101**, 057003 (2008).

[7] E. C. Blomberg, M. A. Tanatar, R. M. Fernandes, I. I. Mazin, B. Shen, Hai-Hu Wen, M. D. Johannes, J. Schmalian, and R. Prozorov, Sign-reversal of the in-plane resistivity anisotropy in hole-doped iron pnictides, Nat. Commun. **4**, 1914 (2013).

[8] Q. Fan, W. H. Zhang, X. Liu, Y. J. Yan, M. Q. Ren, R. Peng, H. C. Xu, B. P. Xie, J. P. Hu, T. Zhang, and D. L. Feng, Plain s-wave superconductivity in single-layer FeSe on $SrTiO_3$ probed by scanning tunneling microscopy, Nat. Phys. **11**, 946 (2015).

[9] H. Kontani and S. Onari, Orbital-Fluctuation-Mediated Superconductivity in Iron Pnictides: Analysis of the Five-Orbital Hubbard-Holstein Model, Phys. Rev. Lett. **104**, 157001 (2010).

[10] H. Kontani, Y. Inoue, T. Saito, Y. Yamakawa, and S. Onari, Orbital fluctuation theory in iron-based superconductors: s_{++}-wave superconductivity, structure transition, and impurity-induced nematic order, Solid State Commun. **152**, 718 (2012).

[11] T. Saito, S. Onari, and H. Kontani, Orbital fluctuation theory in iron pnictides: Effects of As-Fe-As bond angle, isotope substitution, and Z^2-orbital pocket on superconductivity, Phys. Rev. B **82**, 144510 (2010).

[12] Y. J. Yan, W. H. Zhang, M. Q. Ren, X. Liu, X. F. Lu, N. Z. Wang, X. H. Niu, Q. Fan, J. Miao, R. Tao, B. P. Xie, X. H. Chen, T. Zhang, and D. L. Feng, Surface electronic structure and plain s-wave superconductivity of $(Li_{0.8}Fe_{0.2})$OHFeSe revealed by scanning tunneling microscopy, Phys. Rev. B **94**, 134502 (2016).

[13] A. Iyo, K. Kawashima, T. Kinjo, T. Nishio, S. Ishida, H. Fujihisa, Y. Gotoh, K. Kihou, H. Eisaki, and Y. Yoshida, New-Structure-Type Fe-Based Superconductors: $CaAFe_4As_4$ (A = K, Rb, Cs) and $SrAFe_4As_4$ (A = Rb, Cs), J. A. Chem. Soc. **138**, 3410 (2016).

[14] T. Kong, F. F. Balakirev, W. R. Meier, S. L. Bud'ko, A. Gurevich, and P. C. Canfield, Anisotropic magnetoresistance and upper critical fields up to 63 T in $CaKFe_4As_4$ single crystals, arXiv:1606.02241v1.

[15] Z.-C. Wang, C.-Y. He, S.-Q. Wu, Z.-T. Tang, Y. Liu, A. Ablimit, Q. Tao, C.-M. Feng, Z.-A. Xu, and G.-H. Cao, Superconductivity at 35 K by self doping in $RbGd_2Fe_4As_4O_2$, arXiv:1606.08161v2.

[16] D. Mou, T. Kong, W. R. Meier, Felix Lochner, L.-L. Wang, Q. Lin, Y. Wu, S. L. Bud'ko, I. Eremin, D. D. Johnson, P. C. Canfield, and A. Kaminski, Enhancement of the Superconducting Gap by Nesting in $CaKFe_4As_4$– A New High Temperature Superconductor, Phys. Rev. Lett. **117**, 277001 (2016).

[17] G. Li, W. Z. Hu, J. Dong, Z. Li, P. Zheng, G. F. Chen, J. L. Luo, and N. L. Wang, Probing the Superconducting Energy Gap from Infrared Spectroscopy on a $Ba_{0.6}K_{0.4}Fe_2As_2$ Single Crystal with $T_c = 37$ K, Phys. Rev. Lett. **101**, 107004 (2008).

[18] Y. M. Dai, B. Xu, B. Shen, H. H. Wen, X. G. Qiu, and R. P. S. M. Lobo, Optical conductivity of $Ba_{0.6}K_{0.4}Fe_2As_2$: The effect of in-plane and out-of-plane doping in the superconducting gap, Europhys. Lett. **104**, 47006 (2013).

[19] A. A. Schafgans, B. C. Pursley, A. D. Laforge, A. S. Sefat, D. Mandrus, and D. N. Basov, Phonon splitting and anomalous enhancement of infrared-active modes in $BaFe_2As_2$, Phys. Rev. B **84**, 052501 (2011).

[20] B. Xu, Y. M. Dai, B. Shen, H. Xiao, Z. R. Ye, A. Forget, D. Colson, D. L. Feng, H. H. Wen, C. C. Homes, X. G. Qiu, and R. P. S. M. Lobo, Anomalous phonon redshift in K-doped $BaFe_2As_2$ iron pnictides, Phys. Rev. B **91**, 104510 (2015).

[21] G. Q. Huang, Z. W. Xing, and D. Y. Xing, Spin-phonon coupling and effect of pressure in the superconductor LiFeAs: Lattice dynamics from first-principles calculations, Phys. Rev. B **82**, 014511 (2010).

[22] C. C. Homes, M. Reedyk, D. A. Crandles, and T. Timusk, Technique for measuring the reflectance of irregular, submillimeter-sized samples, Appl. Opt. **32**, 2976 (1993).

[23] Y.-M. Dai, B. Xu, B. Shen, H. Xiao, R. P. S. M. Lobo, and X.-G. Qiu, Evolution of the 251 cm^{-1} infrared phonon mode with temperature in $Ba_{0.6}K_{0.4}Fe_2As_2$, Chin. Phys. B **21**, 077403 (2012).

[24] R. Yang, B. Xu, Y. Dai, W. Zhang, J. Liu, Z. Qiu, and X. Qiu, Optical study of the antiferromagnetic ordered state in electron-overdoped $Ca_{0.77}Nd_{0.23}FeAs_2$, Phys. Rev. B **93**, 245110 (2016).

[25] D. Wu, N. Barišić, P. Kallina, A. Faridian, B. Gorshunov, N. Drichko, L. J. Li, X. Lin, G. H. Cao, Z. A. Xu, N. L. Wang, and M. Dressel, Optical investigations of the normal and superconducting states reveal two electronic subsystems in iron pnictides, Phys. Rev. B **81**, 100512 (2010).

[26] C. C. Homes, Y. M. Dai, J. S. Wen, Z. J. Xu, and G. D. Gu, $FeTe_{0.55}Se_{0.45}$: A multiband superconductor in the clean and dirty limit, Phys. Rev. B **91**, 144503 (2015).

[27] Y. M. Dai, H. Miao, L. Y. Xing, X. C. Wang, P. S. Wang, H. Xiao, T. Qian, P. Richard, X. G. Qiu, W. Yu, C. Q. Jin, Z. Wang, P. D. Johnson, C. C. Homes, and H. Ding, Spin-Fluctuation-Induced Non-Fermi-Liquid Behavior with Suppressed Superconductivity in $LiFe_{1-x}Co_xAs$, Phys. Rev. X **5**, 031035 (2015).

[28] D. Fang, X. Shi, Z. Du, P. Richard, H. Yang, X. X. Wu, P. Zhang, T. Qian, X. Ding, Z. Wang, T. K. Kim, M. Hoesch, A. Wang, X. Chen, J. Hu, H. Ding, and H.-H. Wen, Observation of a Van Hove singularity and implication for strong-coupling induced Cooper pairing in KFe_2As_2, Phys. Rev. B **92**, 144513 (2015).

[29] Since phonon A is very weak and merged into the background at high temperatures (>200 K), its position at 295 K is estimated by the anharmonic fitting.

[30] V. G. Hadjiev, M. N. Iliev, K. Sasmal, Y.-Y. Sun, and C. W. Chu, Raman spectroscopy of RFeAsO (R = Sm, La), Phys. Rev. B **77**, 220505(R) (2008).

[31] K.-Y. Choi, Yu. G. Pashkevich, K. V. Lamonova, H. Kageyama, Y. Ueda, and P. Lemmens, Strong anharmonicity and spin-phonon coupling in the quasi-two-dimensional quantum spin system $Sr_{1-x}Ba_xCu_2(BO_3)_2$, Phys. Rev. B **68**, 104418 (2003).

[32] C. C. Homes, S. V. Dordevic, A. Gozar, G. Blumberg, T. Rõõm, D. Hüvonen, U. Nagel, A. D. LaForge, D. N. Basov, and H. Kageyama, Infrared spectra of the low-dimensional quantum magnet $SrCu_2(BO_3)_2$: Measurements and *ab initio* calculations, Phys. Rev. B **79**, 125101 (2009).

[33] A. B. Kuzmenko, L. Benfatto, E. Cappelluti, I. Crassee, D. van der Marel, P. Blake, K. S. Novoselov, and A. K. Geim, Gate Tunable Infrared Phonon Anomalies in Bilayer Graphene, Phys. Rev. Lett. **103**, 116804 (2009).

[34] C. C. Homes, Y. M. Dai, J. Schneeloch, R. D. Zhong, and G. D. Gu, Phonon anomalies in some iron telluride materials, Phys. Rev. B **93**, 125135 (2016).

[35] U. Fano, Effects of configuration interaction on intensities and phase shifts, Phys. Rev. **124**, 1866 (1961).

[36] P. G. Klemens, Anharmonic decay of optical phonons, Phys. Rev. **148**, 845 (1966).

[37] N. L. Wang, W. Z. Hu, Z. G. Chen, R. H. Yuan, G. Li, G. F. Chen, and T. Xiang, High energy pseudogap and its evolution with doping in Fe-based superconductors as revealed by optical spectroscopy, J. Phys.: Condens. Mat. **24**, 294202 (2012).

[38] Z. P. Yin, K. Haule, and G. Kotliar, Magnetism and charge dynamics in iron pnictides, Nat. Phys. **7**, 294 (2011).

[39] C. Zhang, L. W. Harriger, Z. Yin, W. Lv, M. Wang, G. Tan, Y. Song, D. L. Abernathy, W. Tian, T. Egami, K. Haule, G. Kotliar, and P. Dai, Effect of Pnictogen Height on Spin Waves in Iron Pnictides, Phys. Rev. Lett. **112**, 217202 (2014).

[40] Y.-T. Tam, D.-X. Yao, and W. Ku, Itinerancy-Enhanced Quantum Fluctuation of Magnetic Moments in Iron-Based Superconductors, Phys. Rev. Lett. **115**, 117001 (2015).

[41] T. Yoshida, S.-I. Ideta, I. Nishi, A. Fujimori, M. Yi, R. G. Moore, S.-K. Mo, D. Lu, Z.-X. Shen, Z. Hussain, K. Kihou, P. M. Shirage, H. Kito, C.-H. Lee, A. Iyo, H. Eisaki, and H. Harima, Orbital character and electron correlation effects on two- and three-dimensional Fermi surfaces in KFe_2As_2 revealed by angle-resolved photoemission spectroscopy, Front. Phys. **2**, 00017 (2014).

[42] Y. M. Dai, B. Xu, B. Shen, H. Xiao, H. H. Wen, X. G. Qiu, C. C. Homes, and R. P. S. M. Lobo, Hidden T-Linear Scattering Rate in $Ba_{0.6}K_{0.4}Fe_2As_2$ Revealed by Optical Spectroscopy, Phys. Rev. Lett. **111**, 117001 (2013).

[43] W. P. Su, J. R. Schrieffer, and A. J. Heeger, Solitons in Polyacetylene, Phys. Rev. Lett. **42**, 1698 (1979).

[44] R. H. Liu, T. Wu, G. Wu, H. Chen, X. F. Wang, Y. L. Xie, J. J. Ying, Y. J. Yan, Q. J. Li, B. C. Shi, W. S. Chu, Z. Y. Wu, and X. H. Chen, A large iron isotope effect in $SmFeAsO_{1-x}F_x$ and $Ba_{1-x}K_xFe_2As_2$, Nature (London) **459**, 64 (2009).